Received: 27 May 2020 | Revised: 5 September 2020 | Accepted: 28 September 2020

DOI: 10.1111/joa.13337

ORIGINAL PAPER

ANATOMICAL SOCIETY Journal of Anatomy WILEY

Cortical parameters predict bone strength at the tibial diaphysis, but are underestimated by HR-pQCT and μCT compared to histomorphometry

Florian Schmidutz[1,2,3] | Stefan Milz[4] | Damiano Schiuma[1] | Robert G. Richards[1] | Markus Windolf[1] | Christoph M. Sprecher[1]

[1]AO Research Institute Davos, Davos, Switzerland

[2]Department of Orthopaedic Surgery, University of Munich (LMU), Munich, Germany

[3]University of Tübingen, BG Trauma Center, Tübingen, Germany

[4]Department of Anatomy II, University of Munich (LMU), Munich, Germany

Correspondence
Florian Schmidutz, BG Klinik Tübingen/ Eberhard Karls University Tübingen, Schnarrenbergstrasse 95, 72076 Tübingen, Germany.
Email: fschmidutz@bgu-tuebingen.de

Funding information
AO Research Institute Medical Research Fellowship Program

ABSTRACT

Cortical bone and its microstructure are crucial for bone strength, especially at the long bone diaphysis. However, it is still not well-defined how imaging procedures can be used as predictive tools for mechanical bone properties. This study evaluated the capability of several high-resolution imaging techniques to capture cortical bone morphology and assessed the correlation with the bone's mechanical properties. The microstructural properties (cortical thickness [Ct.Th], porosity [Ct.Po], area [Ct.Ar]) of 11 female tibial diaphysis (40–90 years) were evaluated by dual-energy X-ray absorptiometry (DXA), high-resolution peripheral-quantitative-computed-tomography (HR-pQCT), micro-CT (μCT) and histomorphometry. Stiffness and maximal torque to failure were determined by mechanical testing. *T*-Scores determined by DXA ranged from 0.6 to −5.6 and a lower *T*-Score was associated with a decrease in Ct.Th ($p \leq 0.001$) while the Ct.Po ($p \leq 0.007$) increased, and this relationship was independent of the imaging method. With decreasing *T*-Score, histology showed an increase in Ct.Po from the endosteal to the periosteal side ($p = 0.001$) and an exponential increase in the ratio of osteons at rest to those after remodelling. However, compared to histomorphometry, HR-pQCT and μCT underestimated Ct.Po and Ct.Th. A lower *T*-Score was also associated with significantly reduced stiffness ($p = 0.031$) and maximal torque ($p = 0.006$). Improving the accuracy of Ct.Po and Ct.Th did not improve prediction of the mechanical properties, which was most closely related to geometry (Ct.Ar). The ex-vivo evaluation of mechanical properties correlated with all imaging modalities, with Ct.Th and Ct.Po highly correlated with the *T*-Score of the tibial diaphysis. Cortical microstructural changes were underestimated with the lower resolution of HR-pQCT and μCT compared to the histological 'gold standard'. The increased accuracy did not result in an improved prediction for local bone strength in this study, which however might be related to the limited number of specimens and thus needs to be evaluated in a larger collective.

KEYWORDS

bone strength, cortical porosity, partial volume effect, resolution, thickness

1 | INTRODUCTION

The direct relationship between the mechanical properties of specific skeletal regions and their intrinsic architecture has been described by several reports (Hernandez et al., 2006; Imamura et al., 2019; Liu et al., 2010; Ramchand & Seeman, 2018). In particular, cortical bone and its microstructural bone remodelling, as well as the cortical porosity (Ct.Po) and the cortical thickness (Ct.Th), have significant importance for osteoporotic bone loss and mechanical stability (Bala et al., 2014; Imamura et al., 2019; Ohlsson et al., 2017; Zebaze et al., 2019). Microstructural differences offer the opportunity to identify individuals in groups with comparable bone mineral density (BMD) who are at risk for a low-energy trauma fracture (Nishiyama et al., 2012; Skedros et al., 2016; Vico et al., 2008). Further studies have shown that changes in cortical microarchitecture can be independent of the areal BMD (aBMD) measured by dual-energy X-ray absorptiometry (DXA) in patients with fragility fractures (Mussawy et al., 2017; Sornay-Rendu et al., 2007). In addition, the cortical area (Ct.Ar) of the bone was found to predict incidental fractures in older men whereas the aBMD was not (Ohlsson et al., 2017).

Assessing the microstructural parameters of cortical bone has recently become possible in living humans with radiological techniques such as high-resolution peripheral-quantitative-computed-tomography (HR-pQCT). Additionally, ex-vivo investigations such as high resolution micro-computed tomography (μCT) and histology, which is considered the "gold-standard", are viable alternatives. However, neither technique, is suitable for living patients, as they are either destructive or only investigate small bone samples (Palacio-Mancheno et al., 2014). Nevertheless, high-resolution imaging such as μCT and HR-pQCT have advantages over histology. Beyond the determination of microarchitectural parameters, calibration allows the determination of bone mass (Bouxsein et al., 2010) or the mineral weight per tissue volume. Furthermore, specimens are evaluated non-destructively in 3D, making it easy to evaluate larger regions without tedious embedding in polymethylmethacrylate (PMMA). This process enables further investigation in terms of biomechanical testing after microstructural analysis with high resolution CT or clinical follow-up of patients after in-vivo analysis using HR-pQCT.

Fully automatic image analysis algorithms have been suggested based on a dual threshold that allows extraction of cortical and trabecular compartments (Buie et al., 2007). In-vivo, adapted, automated methods have been validated for measurement of Ct.Po (Nishiyama et al., 2010) and the reproducibility of quantitative cortical bone indices based on automated segmentation from HR-pQCT images has been extensively assessed (Burghardt et al., 2010b). Imaging techniques with even higher resolution, such as μCT, may further bridge the findings from HR-pQCT. However, when comparing different imaging techniques, the accuracy of Ct.Po parameters seems to be significantly dependent on the spatial resolution defined by the size of the voxels. Recent studies suggested that a substantial number of cortical pores are undetected as a lower resolution does not allow to capture pores with a small diameter (Tjong et al., 2012). Studies comparing HR-pQCT imaging versus μCT allowing a higher resolution in the detection of Ct.Po are still rare. Moreover, it remains unclear how well X-ray image-derived techniques from a predominately cortical bone skeletal region translate into each other or into classical bone histomorphometry.

Therefore, the aim of this study was first to determine the microstructural properties (cortical thickness [Ct.Th], porosity [Ct.Po], area [Ct.Ar]) and evaluate whether they can be determined accurately by HR-pQCT and μCT compared to the gold standard histomorphometry. Second, how well aBMD derived from local tibial DXA measurements represents those parameters and third, whether the underlying microstructural parameters translate equally into local bone strength.

2 | METHODS

2.1 | Specimen baseline characteristics and evaluation

Eleven left tibiae (defleshed and frozen at −20°C until preparation) from postmenopausal donors ($n = 11$) were collected from the Department of Pathology, Kantonsspital Basel, Switzerland during post mortem dissections with appropriate consent of the relatives. The specimens had already been used and biomechanically evaluated in a previous study (Popp et al., 2012), and were stored in polyethylene bags at −20°C at the AO Research Institute, Davos, Switzerland. All measurements were performed within 24 h after thawing the specimens to room temperature and immediately refrozen upon completion. Conventional X-rays had been taken from all tibiae prior to processing to exclude possibly unreported alterations of the tibiae.

Evaluation of the tibial bone morphology was started 122.5 mm proximal to the distal tibia endplate as (Figure 1a). The DXA measurements were performed over a length of 40 mm, HR-pQCT over 9 mm, μCT over 6 mm and histomorphometry was performed from three histological sections at 2, 4 and 6 mm (Figure 1).

2.2 | DXA and *T*-Score

The *T*-Score for the distal tibial diaphysis was obtained by DXA (Figure 1a). Scans were obtained by placing the defrosted vacuum-packed tibial preparations in a basin filled with semolina, to simulate soft tissue, using a standard DXA device (Hologic QDR 4500 A™, Hologic). The manufacturer's software was used according to a previously described standardized procedure for analysing the tibial diaphysis (Casez et al., 1994). Briefly, the region of interest (ROI) for the tibial diaphysis started 130 mm from the distal tibia endplate and included a total length of 40 mm of the long bone

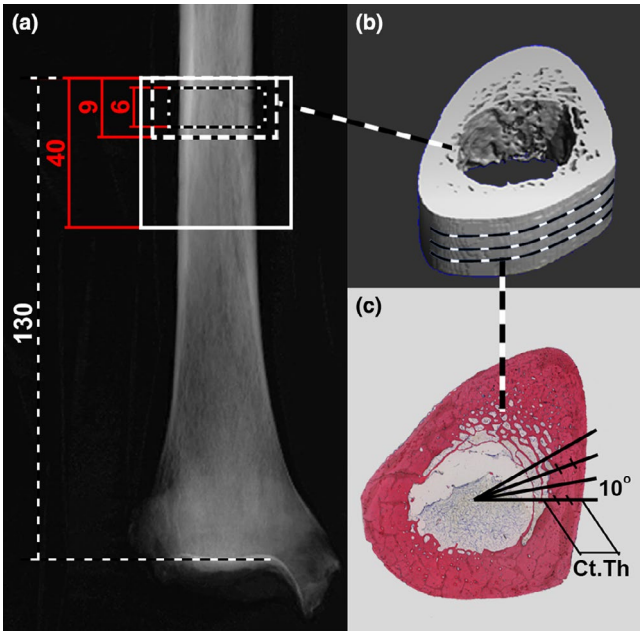

FIGURE 1 Tibial bone morphology was determined starting 130 mm from the distal tibia endplate running from proximal to distal: (a) DXA was performed over a length of 40 mm (white rectangle), HR-pQCT over a length of 9 mm (white dotted line) and µCT over a length of 6 mm (black dotted line). (b) 3D reconstruction of the µCT showing the level of the three histological sections (2, 4, 6 mm). (c) Histomorphometry was performed at the periosteal, central and endosteal regions which were defined by dividing the cortical thickness (Ct.Th) every 10 degrees in three regions

axis running from proximal to distal (Figure 1a; Popp et al., 2009). The *T*-scores were calculated as the number of standard deviations from the mean peak bone mass of a female reference population of 400 healthy Caucasians living in the area of Bern, Switzerland. Peak bone mass (mean value ± *SD*) of this female reference population is 1.278 ± 0.116 g/cm^2 at the distal tibial diaphysis (Popp et al., 2009).

2.3 | HR-pQCT

Cut diaphysis specimens were positioned in a carbon fibre shell and subjected to HR-pQCT measurement (XtremeCT™, Scanco Medical). The X-ray tube was set at 60 kVp and 900 µA. The SCANCO phantom was scanned daily for quality control. The isotropic voxel had a length of 82 µm. The scanned VOI was defined on a scout view and represented the total length of the most proximal 9 mm along the bone axis of diaphysis (Figure 1a). Each VOI was semi-automatically segmented into cortical bone using a threshold-based algorithm. The cortical bone was segmented with ranges of 600–1500 mgHA/cm^3 (Laib & Ruegsegger, 1999; Popp et al., 2009). Parameters of interest were Ct.Th, Ct.Po and Ct.Ar, which were calculated using an automated image processing chain (Burghardt, Buie et al., 2010; Burghardt, Kazakia et al., 2010).

2.4 | µCT measurements

All specimens were subjected to µCT measurements (µCT 40, Scanco Medical). The SCANCO phantom was scanned daily for quality control. The X-ray tube was set at 70 kVp and 114 µA, and the isotropic voxel size was 36 µm. The analysed volume in the diaphysis was defined on a scout view, with a total length of 6 mm (Figure 1b) and was located in the centre of the volume scanned by HR-pQCT. Each volume was semi-automatically segmented into cortical bone using the ranges of 512–1,500 mgHA/cm^3 (Laib et al., 1997; Laib & Ruegsegger, 1999). The threshold values were optimized in accordance with the density histograms of the specimens. The cortical bone volume was used to analyse the porosity of the cortex. The parameters of interest were Ct.Th, Ct.Po and Ct.Ar.

2.5 | Biomechanical testing

All eleven tibiae had been tested biomechanically in a previous study at the diaphysis for mechanical strength by Popp et al. (Popp et al., 2012). Briefly, the specimens were embedded in PMMA on both ends for torsional testing on a servo hydraulic material testing machine (MTS 858 Mini-Bionix II; MTS Systems Inc.). Torsional stiffness was calculated as slope of the torque-angle curve. The maximal torque was defined as torque at failure.

2.6 | Histological evaluation and histomorphometry

For histological preparation, all specimens were fixed in 70% ethanol for 10 days. The bone was dehydrated in increasing concentrations of ethanol (50%, 70%, 96% and 100%), defatted in Xylene and embedded in PMMA. Of each sample, three sections at the 2-, 4- and 6-mm levels were taken using a saw-microtome (Leica SP 1600™, Leica). The 200-µm thick sections were ground and polished to a final thickness of 100 ± 20 µm and then stained with Giemsa-Eosin. All stained sections underwent a histological investigation and were digitalized using an Axiovert200 m with a motorized stage (Zeiss) equipped with an AxioCam HRc (Zeiss) using the Mosaix function of the Axiovision software (version 4.8.3, Zeiss) with a pixel size of 3.77 µm (10x objective).

In the histomorphometric analysis the intramedullary canal was manually defined. Quantitative analysis was performed on a computer workstation equipped with Zeiss KS400™ image analysis software (Zeiss) in a semiautomatic segmentation process. The Ct.Th was measured every 10 degree along a line from the centre of gravity (Figure 1c). This segmentation was additionally used for defining the endosteal, central and periosteal regions.

The outcome parameters (for the histomorphometry on the cortical bone) were Ct.Th, Ct.Po and pore area, which was used to calculate the equivalent/corresponding pore diameter. The osteonal remodelling ratio was calculated as the ratio between the number of osteons at rest (defined as osteon with the inner pore

diameter between 30–50 μm) and the number of still modelling osteons (osteon with an inner pore diameter 100 and 200 μm). The two groups were defined according to (Pazzaglia et al., 2013) who showed that more advanced remodelling was associated with a smaller inner diameter of an osteon, where younger, just recently created osteons that are not yet in a state of advanced remodelling were represented by a larger inner diameter of the Haversian canal.

2.7 | Statistical analysis

Statistical analyses were conducted using SPSS software package (version 22, IBM SPSS). Normality of data distribution was screened and proved with the Shapiro–Wilk test. Correlations were performed using 2-tailed Pearson Correlation test and the outcomes were reported in terms of both *r* coefficient and *p*-value. Parameters of interest (Ct.Th, Ct.Po, Ct.Ar) and regions (periosteal, cortical, endosteal) generated by the different methods (HR-pQCT, uCT, histology) were compared using a General Linear Model Repeated Measures test (repeated measures analysis of variance [ANOVA]). Bonferroni Post Hoc test was applied to adjust for multiple comparisons. The significance level was set at $p = 0.05$ for all statistical tests.

3 | RESULTS

3.1 | Characteristics and *T*-Score of the donor tibiae

The mean age of the 11 female donors was 74 ± 14 years (mean ± *SD*) with a mean height of 162 ± 9 cm and weight of 58 ± 6 kg giving a body-mass-index of 22 ± 2 kg/m^2. DXA revealed a mean *T*-Score of −2.2 (Table 1).

The mean Ct.Th was 2.6 ± 0.7 mm with HR-pQCT, 2.5 ± 0.7 mm with μCT and 4.1 ± 0.9 with histomorphometry. Significant differences for the Ct.Th results were observed with histomorphometry compared to values obtained with either CT technique (uCT $p < 0.001$; HR-pQCT $p < 0.001$). The mean Ct.Po was 0.5 ± 0.5% with HR-pQCT, 6.6 ± 6.5% with μCT and 17.1 ± 10.3% with histomorphometry. Significant differences for the Ct.Po results were observed with histomorphometry compared to values obtained with either CT technique (uCT $p = 0.001$; HR-pQCT $p = 0.001$). For both microstructural parameters (Ct.Th and Ct.Po), histomorphometry revealed greater cortical thickness and porosity compared to the imaging modalities (μCT and HR-pQCT).

The mean Ct.Ar was of 196 ± 52 mm^2 with HR-pQCT, 193 ± 53 mm^2 with μCT and 215 ± 38 mm^2 with histomorphometry. The Ct.Ar results of the histomorphometry were significantly different to those of the uCT ($p = 0.031$) while the results of the HR-pQCT did not reach significance ($p = 0.056$).

3.2 | Histological evaluation and histomorphometry

Qualitative evaluation of the bone in histological sections did not show pathological alteration and the vast majority of the osteocyte lacunas contained cell nuclei, indicative for living bone. Distinct regional differences in cortical thickness, cortical porosity and the Haversian canals were observed in sections of donors with different *T*-Scores (Figure 2a–c).

Quantitative histomorphometric analysis of cortical porosity in the cross-sectional areas revealed a strong decrease from the endosteal towards the periosteal regions (Figure 3). Significant differences between the endosteal and the central regions ($p = 0.002$) as well as between the endosteal and the periosteal region ($p = 0.001$) were found using a 'General Linear Model Repeated Measures' with Bonferroni correction. No significant difference was detected between the periosteal and central regions ($p = 0.204$; Figure 3). The osteonal pore size was determined and used to calculate osteonal remodelling as the ratio between the number of osteons at rest (pore Ø 30–50 μm) and the number of still modelling osteons (Ø 100–200 μm). In cases with an increase in Co.Pt the osteonal remodelling ratio decreased extensively and this relationship is shown in Figure 4.

TABLE 1 Donor characteristics

Donor no	Age (years)	Height (cm)	Weight (kg)	BMI (kg/m^2)	*T*-score
1	40	161	52	20.1	−0.9
2	88	157	61	24.7	−1.7
3	90	158	54	21.6	−1.9
4	74	170	63	21.8	−1.3
5	74	180	63	19.4	0.6
6	61	163	66	24.8	−2.2
7	84	164	63	23.4	−5.3
8	76	155	51	21.2	−5.6
9	84	164	56	20.8	−4.2
10	71	156	63	25.9	−0.3
11	72	149	50	22.5	−0.9
Mean ± SD Range (min–max)	74 ± 14 (40–90)	162 ± 9 (149–180)	58 ± 6 (50–66)	22 ± 2 (19.4–25.9)	−2.2 ± 1.9 (−5.6 to 0.6)

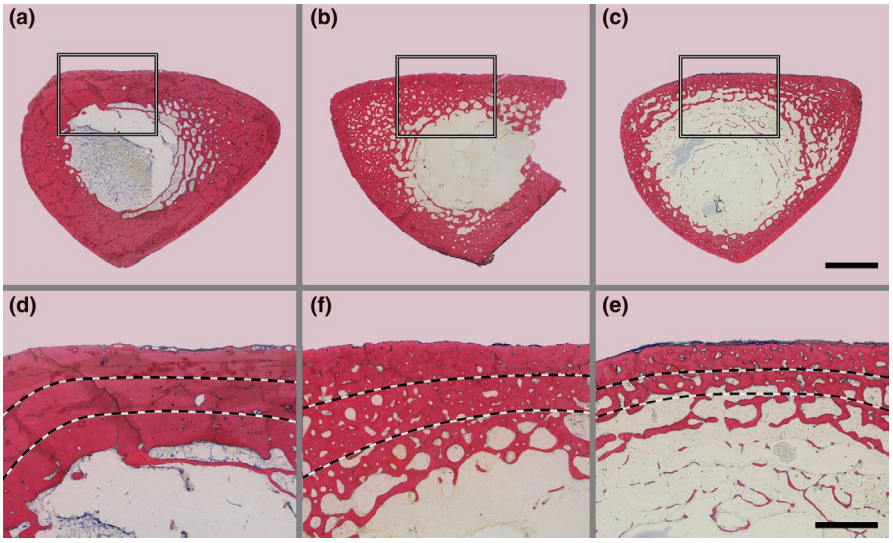

FIGURE 2 Three histological tibia cross-sections (Giemsa-Eosin) of representative specimens with decreasing BMD: (a/d) Donor 1/*T*-Score −0.9; (b/e) Donor 2/*T*-Score −1.7 and (c/f) Donor 8/*T*-Score −5.6. Cortical thickness (a: 4.6 ± 1.4 mm, b: 4.6 ± 1.6, c: 3.2 ± 1.5) decreases with a lower *T*-Score, while cortical porosity concurrently increases (a: 3.3%, b: 13.4%, c: 25.3%). The higher magnification images (d–f) demonstrate that the increase in cortical porosity is more pronounced in the endosteal region than in the periosteal region. Cortical regions (endosteal, cortical, periosteal) are separated with dashed lines (scalebar: a–c = 5 mm and d–f = 2 mm)

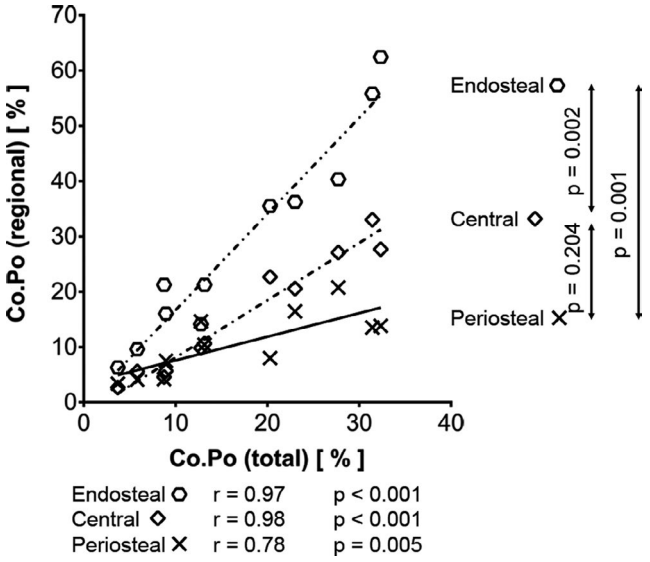

FIGURE 3 Cortical porosity (Ct.Po) in the three cortical regions (endosteal, cortical and periosteal) determined by histomorphometry. Significant higher Ct.Po was measured in the endosteal region compared to the central and periosteal region, which was more pronounced with a lower *T*-Score. The Ct.Po of all regions showed a high and significant correlation with the total Ct.Po ($r = 0.78–0.98$)

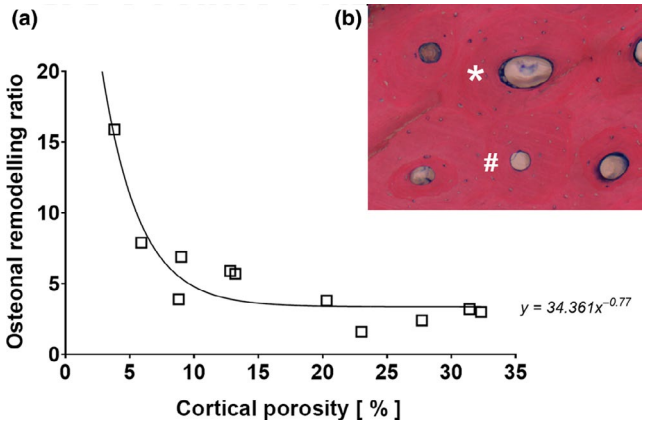

FIGURE 4 Osteonal pore size and cortical porosity derived from histomorphometry (Giemsa-Eosin): a) Osteonal pore size was used to calculate osteonal remodeling as the ratio between the number of osteons at rest (pore Ø 30 - 50 µm, #) and the number of still modelling osteons (Ø 100 - 200 µm, *). b) The osteonal remodelling ratio highly decreased with increasing cortical porosity

3.3 | Correlations with *T*-Score

The biomechanical testing of torsional stiffness ($r = 0.77$; $p = 0.006$) and maximal torque ($r = 0.65$; $p = 0.031$) revealed a significant positive correlation with the *T*-Score (Figure 5a,b). Correlation between torsional stiffness and maximal torque also revealed a significant positive correlation ($r = 0.76$; $p = 0.007$; Figure 5c).

The Ct.Th showed a strong or very strong and significant positive correlation with the *T*-Score, irrespective of the imaging modality used (HR-pQCT, µCT and histomorphometry, Figure 5d).

Cortical porosity had significant negative correlations with the *T*-Scores for all three imaging modalities used (Figure 5e). µCT ($r = −0.76$) and histomorphometry ($r = −0.80$) had strong or very strong correlations, whereas HR-pQCT ($r = −0.57$) only had a moderate correlation (Figure 5e).

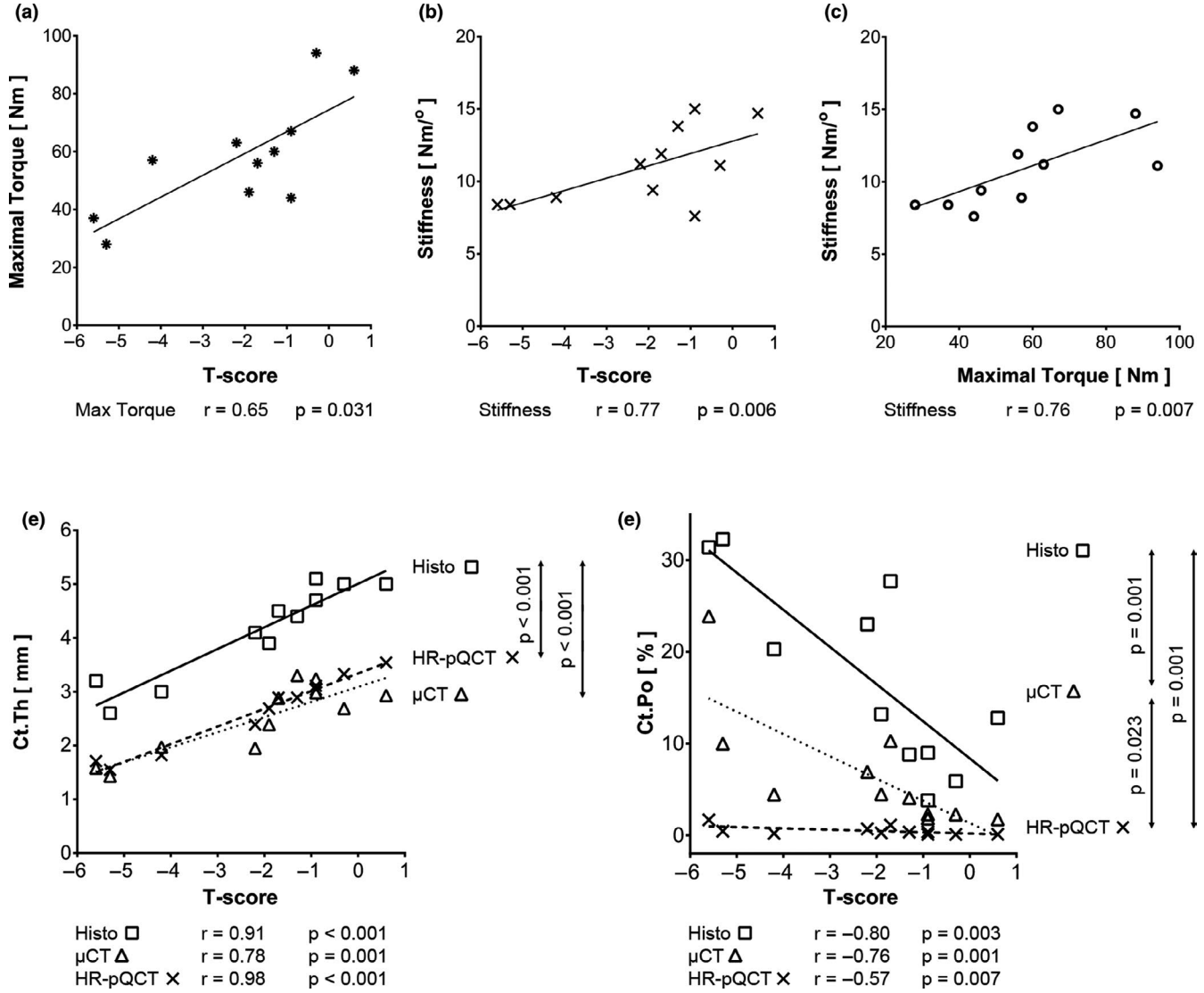

FIGURE 5 Biomechanical parameters([a]; [b]; [c]) and morphometric parameters ([d]; [e]) determined at the distal tibia. Correlations in almost all parameters were strong ($0.6 < r < 0.8$) or very strong ($0.8 \leq r < 1.0$) with the tibial *T*-Score (DXA). Correlations among the biomechanical parameters of (a) stiffness and (b) maximal torque were lower compared to the morphometric parameters of (d) cortical thickness (Ct.Th) and (e) cortical porosity (Ct.Po) determined by histomorphology and µCT. Cortical porosity correlated with a higher degree with a higher resolution imaging modality applied. Stiffness correlated well with the maximal torque (c)

Furthermore, the histomorphometry results for Ct.Po showed a stronger correlation with the *T*-Score compared to µCT and HR-pQCT (Figure 5).

3.4 | Correlation of the microstructural and mechanical parameters

The Ct.Th, Ct.Po and Ct.Ar of the tibial diaphysis were correlated with maximal torque and stiffness (Table 2). The strongest correlations were found consistently for the Ct.Ar and maximal torque and stiffness (r = 0.62–0.79), with histomorphometry demonstrating stronger correlations compared with uCT and HR-pQCT. Similarly, but at a lower level Ct.Th correlated with the maximal torque at failure (r = 0.49–0.74), which reached statistical significance for HR-pQCT ($p = 0.009$) and histomorphometry ($p = 0.021$) but not for µCT ($p = 0.123$). A consistent trend for the negative correlations between Ct.Po and the maximal torque (r = −0.43 to −0.56) as well as stiffness (r = −0.18 to −0.40) was found but did not reach statistical significance (p = 0.076–0.59).

4 | DISCUSSION

This study evaluated the ability of different imaging modalities to assess the microstructural architecture of the tibial cortex and how these parameters translate into bone strength. The distal tibia was chosen because its cortical microstructural architecture can be evaluated with HR-pQCT in patients and allows direct translation of the measured parameters into local bone

TABLE 2 Correlation *r* and significance (*p*) between the parameters of the cortex and local bone strength at the tibial diaphysis

	Cortical thickness (Ct.Th)			Cortical porosity (Ct.Po)			Cortical area (Ct.Ar)		
	HR-pQCT	µCT	Histology	HR-pQCT	µCT	Histology	HR-pQCT	µCT	Histology
Stiffness	0.62 (0.041)	0.57 (0.069)	0.54 (0.084)	−0.18 (0.594)	−0.40 (0.223)	−0.34 (0.302)	0.74 (0.009)	0.62 (0.040)	0.76 (0.007)
Maximal torque	0.74 (0.009)	0.49 (0.123)	0.68 (0.021)	−0.43 (0.188)	−0.56 (0.076)	−0.55 (0.077)	0.78 (0.004)	0.74 (0.009)	0.79 (0.004)

strength owing to its high share of cortical bone (Popp et al., 2012).

The results demonstrate that Ct.Th, Ct.Po and Ct.Ar measured by HR-pQCT and µCT were highly comparable, indicating that the higher X-ray based resolution of the quantitative CT modality had a very limited impact on the results. Similarly, the correlation of HR-pQCT and µCT derived cortical parameters to maximal torque were comparable. In contrast, the microstructural parameters obtained from the histological sections revealed significant and systematic differences compared to the X-ray based methods used with at the resolution of 82 µm for HR-pQCT and 36 µm µCT. All values for Ct.Th and Ct.Po were numerically higher when assessed with histomorphometry, with Ct.Po being up to three times lower when measured by HR-pQCT and µCT. However, it has to be mentioned that meanwhile micro-CT resolution of less than 5 µm are available, which might narrow the differences beetwen the measurement modalities. Cooper et al. could demonstrate that a higher resolution of <10 µm is required to consistently detect all cortical pores (Cooper et al., 2004, 2007), while in this study resolutions of 82 µm for HR-pQCT and 36 µm µCT were used.

The lower values obtained for Ct.Th and Ct.Po by the X-ray based methods can be attributed to the partial volume effect (Figure 6), which is inversely related to voxel size (Kamer et al., 2016; Palacio-Mancheno et al., 2014; Tjong et al., 2012). It is thus not surprising that the results derived from histological evaluation, often still considered the 'gold standard', are the least affected due to the very high resolution and the very small volume from which the information is derived (Kamer et al., 2016; Palacio-Mancheno et al., 2014). Therefore, the highest differences can particularly be observed for Ct.Po, which has a large heterogeneity in the pore size and thus cannot be fully detected with a lower resolution. Parameters, such as Ct.Th, which have relatively few voxels at the edge, are less severely affected than Ct.Po, with a relatively large number of voxels at the edges (Kamer et al., 2016). Thus, large pores tend to be underestimated and smaller pores can even be missed despite the high resolution of µCT (Schoenau et al., 2002). This results in underestimation of total Ct.Po as previously described by Zebaze et al. (2010, 2019) and demonstrated by Tjong et al. in a resolution based HR-pQCT study (Tjong et al., 2012). Similarly, our and other results show that HR-pQCT (Longo et al., 2017; Scharmga et al., 2016) and even µCT underestimates microstructural parameters, especially Ct.Po, compared to histomorphometry. Again, the increasing higher resolutions of micro-CTs might influence these differences and lead to comparable results.

In this study, the more accurate determination of the Ct.Po by histology failed to produce better correlations with mechanical parameters such as the maximal torque or stiffness and did not reach significance for all three methods. Similarly, Ct.Th revealed only a moderate correlation with the mechanical parameters and reached significance only for the values obtained by HR-pQCT. Correlating the Ct.Th of the different measurement methods with the parameters of strength keeps some uncertainty and might be more likely related to the sample size rather than significant differences among

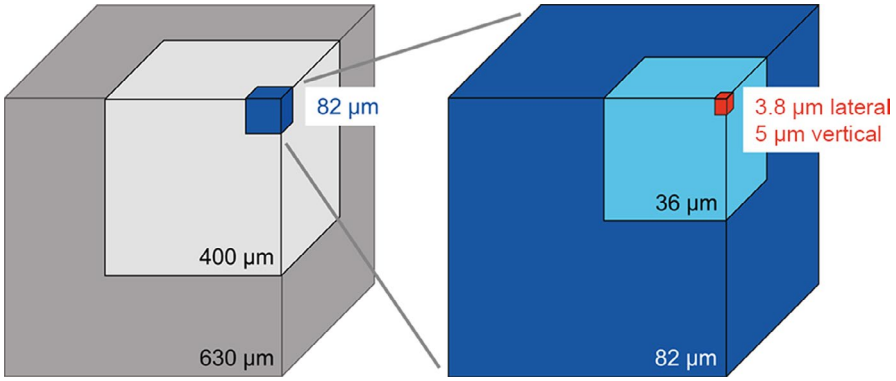

FIGURE 6 Schematic drawing demonstrating the'partial volume effect' with respect to the volume and resolution used. Clinical CT ranging from 400 to 630 µm resolution (dark and middle gray), high resolution µCT with 36 µm and HR-pQCT with 82 µm resolution (light and dark blue) in comparison to the microscopic 3.8 µm lateral/5 µm vertical resolution of the histological Giemsa Eosin sections (red)

the techniques applied. Nevertheless, also differences in the segmentation methods and determination of the so-called transitional zone, corresponding to the trabecularized endosteal cortical bone, might have influenced the results. The difficulty in identifying the border of the cortical and trabecular compartments is challenging (Sornay-Rendu et al., 2017; Zebaze et al., 2019) and might also explain differences between the methods applied but also between different studies.

Standardized measurement of cortical microstructural parameters, especially Ct.Po, remains challenging. Beyond the limitations of imaging methods, such as resolution, the reason for this limitation is its site-specificity. Especially the identification and segmentation of the transitional zone is challenging and highly influences the Ct.Po values (Sornay-Rendu et al., 2017), which also is visible in our histological sections (Figure 2).

Ct.Ar correlated highly and consistently with all the techniques for measuring local bone strength. As any structural robustness is basically dependent on the cross sectional area, especially for bending forces, the high correlation of Ct.Ar and local bone strength at the tibial diaphysis is conclusive. The trabecularization of the cortex describes the pathophysiological modus of action of initial cortical bone loss, which may be to be quantified by Ct.Po and could be seen in our analysis.

However, when assessing the perimeter of the long bones, i.e. the distance to the neutral axis, the contribution of the available bone mass and its distribution over a given cross section to structural robustness is more than the loss of bone mass alone. Ohlsson et al. recently reported that the Ct.Ar, but not cortical porosity, predicted incident fractures independently of the aBMD in older men (Ohlsson et al., 2017).

Although histomorphometry potentially provides higher resolution with more accurate evaluation of microstructural parameters (at the expense of a reduced field of view), we did not find an improved prediction of bone strength, which however can also be related to the limited number of specimens evaluated. Histological sections remain important for understanding the osteoporotic processes. The trabecularization of the cortex was a prominent feature observed in osteoporotic bone when compared to normal bone. A more detailed histological assessment of the periosteal, central and the endosteal regions further enabled identification of osteons at rest and those actively remodelling (Crane et al., 2019; Imamura et al., 2019). In our study, the definition of the two groups of osteons, those at rest and those actively remodelling, was based on arbitrarily defined intervals for the inner osteon diameter (Figure 4). The group of osteons at rest was more or less the endpoint of inner osteon diameter filling. The underlying biological phenomenon was described in detail by (Pazzaglia et al., 2013) who suggested a biological regulation of osteoclast activity by the number of osteocytes and by their cumulative capability to secrete matrix within the spatial limits of the cutting cone of the osteon. Yet our choice of dimensional parameters was already adapted to a future increase in CT scanner resolution, which would allow identification of the more actively remodelling osteon group in patients. This process is not yet feasible with current scanner technology and determination of this parameter still requires histomorphometry.

The present study had certain inherent limitations. All measurements were done ex-vivo and do not necessarily translate into the same findings in-vivo. Only the tibial diaphysis was considered, and the findings may differ when applying a similar methodology to other bones and regions. Bone strength was assessed by biomechanical testing and may not necessarily reflect the forces involved in fragility fractures in patients. Besides, the radiological and histological measurements did not evaluate exactly the same region of interest and were also affected by the destructive biomechanical testing, limiting the comparability of our results. Due to the nature of organ donation, the specimens used for this study were from an elderly population and the donor age range was narrow, which might have biased the results.

In conclusion, we demonstrated that the microstructural parameters of the tibial diaphysis in terms of Ct.Th and Ct.Po highly correlated with the local *T*-Score, and these high correlations were irrespective of the imaging measurement method used. Notably, cortical parameters and especially Ct.Po were underestimated

with high-resolution imaging CT (at the resolution used of 82 μm [HR-pQCT] and 36 μm [μCT]) compared to the 'gold standard' histology which in turn also allowed evaluation of osteonal remodelling activity. The improved analysis of Ct.Po and Ct.Th did not result in an improvement in bone strength prediction, which however needs to be evaluated in a larger collective. Cortical area still translated better into local bone strength indicating size and shape in a single parameter due to the simplicity of the geometry at this skeletal site.

ACKNOWLEDGMENTS

We thank the AO Research Institute Medical Research Fellowship Program for providing assistance and financial support to Dr. F. Schmidutz. The authors thank Dr. A.W. Popp and Mr. M. Bluvol for supporting the project and histological work.

CONFLICT OF INTEREST

The authors declare that there is no conflict of interest.

ETHICAL APPROVAL

All post mortem dissections and procedures were performed with appropriate consent and in accordance with ethical standards of Switzerland and the Declaration of Helsinki.

AUTHOR CONTRIBUTIONS

Study design: F.S. and C.M.S., Data collection: F.S., D.S. and C.M.S., Data analysis and interpretation: F.S., S.M., R.G.R., M.W. and C.M.S., Drafting manuscript: F.S., S.M. and C.M.S., Revising manuscript and approval: All.

ORCID

Florian Schmidutz https://orcid.org/0000-0002-3716-7870

REFERENCES

Bala, Y., Zebaze, R., Ghasem-Zadeh, A., Atkinson, E.J., Iuliano, S., Peterson, J.M. et al. (2014) Cortical porosity identifies women with osteopenia at increased risk for forearm fractures. *Journal of Bone and Mineral Research*, 29(6), 1356–1362. https://doi.org/10.1002/jbmr.2167

Bouxsein, M.L., Boyd, S.K., Christiansen, B.A., Guldberg, R.E., Jepsen, K.J. & Muller, R. (2010) Guidelines for assessment of bone microstructure in rodents using micro-computed tomography. *Journal of Bone and Mineral Research*, 25, 1468–1486.

Buie, H.R., Campbell, G.M., Klinck, R.J., MacNeil, J.A., & Boyd, S.K. (2007) Automatic segmentation of cortical and trabecular compartments based on a dual threshold technique for in vivo micro-CT bone analysis. *Bone*, 41, 505–515.

Burghardt, A.J., Buie, H.R., Laib, A., Majumdar, S. & Boyd, S.K. (2010) Reproducibility of direct quantitative measures of cortical bone microarchitecture of the distal radius and tibia by HR-pQCT. *Bone*, 47, 519–528. https://doi.org/10.1016/j.bone.2010.05.034

Burghardt, A.J., Kazakia, G.J., Ramachandran, S., Link, T.M. & Majumdar, S. (2010) Age- and gender-related differences in the geometric properties and biomechanical significance of intracortical porosity in the distal radius and tibia. *Journal of Bone and Mineral Research*, 25, 983–993.

Casez, J.P., Troendle, A., Lippuner, K. & Jaeger, P. (1994) Bone mineral density at distal tibia using dual-energy X-ray absorptiometry in normal women and in patients with vertebral osteoporosis or primary hyperparathyroidism. *Journal of Bone and Mineral Research*, 9, 1851–1857. https://doi.org/10.1002/jbmr.5650091203

Cooper, D.M., Matyas, J.R., Katzenberg, M.A. & Hallgrimsson, B. (2004) Comparison of microcomputed tomographic and microradiographic measurements of cortical bone porosity. *Calcified Tissue International*, 74, 437–447. https://doi.org/10.1007/s00223-003-0071-z

Cooper, D.M., Thomas, C.D., Clement, J.G., Turinsky, A.L., Sensen, C.W. & Hallgrimsson, B. (2007) Age-dependent change in the 3D structure of cortical porosity at the human femoral midshaft. *Bone*, 40, 957–965. https://doi.org/10.1016/j.bone.2006.11.011

Crane, M.A., Kato, K.M., Patel, B.A. & Huttenlocker, A.K. (2019) Histovariability in human clavicular cortical bone microstructure and its mechanical implications. *Journal of Anatomy*, 235, 873–882. https://doi.org/10.1111/joa.13056

Hernandez, C.J., Gupta, A. & Keaveny, T.M. (2006) A biomechanical analysis of the effects of resorption cavities on cancellous bone strength. *Journal of Bone and Mineral Research*, 21, 1248–1255. https://doi.org/10.1359/jbmr.060514

Imamura, T., Tsurumoto, T., Saiki, K., Nishi, K., Okamoto, K., Manabe, Y. et al. (2019) Morphological profile of atypical femoral fracturs: Age-related changes to the cross-sectional geometry of the diaphysis. *Journal of Anatomy*, 235, 892–902. https://doi.org/10.1111/joa.13060

Kamer, L., Noser, H., Blauth, M., Lenz, M., Windolf, M. & Popp, A.W. (2016) Bone mass distribution of the distal tibia in normal, osteopenic, and osteoporotic conditions: An Ex vivo assessment using HR-pQCT, DXA, and computational modelling. *Calcified Tissue International*, 99, 588–597. https://doi.org/10.1007/s00223-016-0188-5

Laib, A., Hildebrand, T., Hauselmann, H.J. & Ruegsegger, P. (1997) Ridge number density: a new parameter for in vivo bone structure analysis. *Bone*, 21, 541–546.

Laib, A. & Ruegsegger, P. (1999) Calibration of trabecular bone structure measurements of in vivo three-dimensional peripheral quantitative computed tomography with 28-microm-resolution microcomputed tomography. *Bone*, 24, 35–39.

Liu, X.S., Cohen, A., Shane, E., Yin, P. T., Stein, E. M., Rogers, H. et al. (2010) Bone density, geometry, microstructure, and stiffness: Relationships between peripheral and central skeletal sites assessed by DXA, HR-pQCT, and cQCT in premenopausal women. *Journal of Bone and Mineral Research*, 25, 2229–2238.

Longo, A.B., Salmon, P.L. & Ward, W.E. (2017) Comparison of ex vivo and in vivo micro-computed tomography of rat tibia at different scanning settings. *Journal of Orthopaedic Research*, 35, 1690–1698. https://doi.org/10.1002/jor.23435

Mussawy, H., Ferrari, G., Schmidt, F.N., Schmidt, T., Rolvien, T., Hischke, S. et al. (2017) Changes in cortical microarchitecture are independent of areal bone mineral density in patients with fragility fractures. *Injury*, 48, 2461–2465. https://doi.org/10.1016/j.injury.2017.08.043

Nishiyama, K.K., Macdonald, H.M., Buie, H.R., Hanley, D.A. & Boyd, S.K. (2010) Postmenopausal women with osteopenia have higher cortical porosity and thinner cortices at the distal radius and tibia than women with normal aBMD: an in vivo HR-pQCT study. *Journal of Bone and Mineral Research*, 25, 882–890.

Nishiyama, K.K., Macdonald, H.M., Moore, S.A., Fung, T., Boyd, S.K. & McKay, H.A. (2012) Cortical porosity is higher in boys compared with girls at the distal radius and distal tibia during pubertal growth: An HR-pQCT study. *Journal of Bone and Mineral Research*, 27, 273–282.

Ohlsson, C., Sundh, D., Wallerek, A., Nilsson, M., Karlsson, M., Johansson, H. et al. (2017) Cortical bone area predicts incident fractures independently of areal bone mineral density in older men. *Journal of Clinical Endocrinology and Metabolism*, 102, 516–524.

Palacio-Mancheno, P.E., Larriera, A.I., Doty, S.B., Cardoso, L. & Fritton, S.P. (2014) 3D assessment of cortical bone porosity and tissue mineral density using high-resolution microCT: Effects of resolution and threshold method. *Journal of Bone and Mineral Research*, 29, 142–150.

Pazzaglia, U.E., Congiu, T., Pienazza, A., Zakaria, M., Gnecchi, M. & Dell'orbo, C. (2013) Morphometric analysis of osteonal architecture in bones from healthy young human male subjects using scanning electron microscopy. *Journal of Anatomy*, 223, 242–254. https://doi.org/10.1111/joa.12079

Popp, A.W., Senn, C., Franta, O., Krieg, M.A., Perrelet, R. & Lippuner, K. (2009) Tibial or hip BMD predict clinical fracture risk equally well: Results from a prospective study in 700 elderly Swiss women. *Osteoporosis International*, 20, 1393–1399. https://doi.org/10.1007/s00198-008-0808-7

Popp, A.W., Windolf, M., Senn, C., Tami, A., Richards, R.G., Brianza, S. & Schiuma, D. (2012) Prediction of bone strength at the distal tibia by HR-pQCT and DXA. *Bone*, 50, 296–300. https://doi.org/10.1016/j.bone.2011.10.033

Ramchand, S.K. & Seeman, E. (2018) The influence of cortical porosity on the strength of bone during growth and advancing age. *Current Osteoporosis Reports*, 16, 561–572. https://doi.org/10.1007/s11914-018-0478-0

Scharmga, A., Peters, M., van Tubergen, A., van den Bergh, J., de Jong, J., Loeffen, D. et al. (2016) Visual detection of cortical breaks in hand joints: Reliability and validity of high-resolution peripheral quantitative CT compared to microCT. *BMC Musculoskeletal Disorders*, 17, 271. https://doi.org/10.1186/s12891-016-1148-y

Schoenau, E., Neu, C.M., Rauch, F. & Manz, F. (2002) Gender-specific pubertal changes in volumetric cortical bone mineral density at the proximal radius. *Bone*, 31, 110–113. https://doi.org/10.1016/S8756-3282(02)00802-5

Skedros, J.G., Knight, A.N., Pitts, T.C., O'Rourke, P.J. & Burkhead, W.Z. (2016) Radiographic morphometry and densitometry predict strength of cadaveric proximal humeri more reliably than age and DXA scan density. *Journal of Orthopaedic Research*, 34, 331–341. https://doi.org/10.1002/jor.22994

Sornay-Rendu, E., Boutroy, S., Duboeuf, F. & Chapurlat, R.D. (2017) Bone microarchitecture assessed by HR-pQCT as predictor of fracture risk in postmenopausal women: The OFELY study. *Journal of Bone and Mineral Research*, 32, 1243–1251. https://doi.org/10.1002/jbmr.3105

Sornay-Rendu, E., Boutroy, S., Munoz, F. & Delmas, P.D. (2007) Alterations of cortical and trabecular architecture are associated with fractures in postmenopausal women, partially independent of decreased BMD measured by DXA: The OFELY study. *Journal of Bone and Mineral Research*, 22, 425–433. https://doi.org/10.1359/jbmr.061206

Tjong, W., Kazakia, G.J., Burghardt, A.J. & Majumdar, S. (2012) The effect of voxel size on high-resolution peripheral computed tomography measurements of trabecular and cortical bone microstructure. *Medical Physics*, 39, 1893–1903. https://doi.org/10.1118/1.3689813

Vico, L., Zouch, M., Amirouche, A., Frère, D., Laroche, N., Koller, B. et al. (2008) High-resolution pQCT analysis at the distal radius and tibia discriminates patients with recent wrist and femoral neck fractures. *Journal of Bone and Mineral Research*, 23, 1741–1750. https://doi.org/10.1359/jbmr.080704

Zebaze, R., Atkinson, E.J., Peng, Y., Bui, M., Ghasem-Zadeh, A., Khosla, S. & Seeman, E. (2019) Increased cortical porosity and reduced trabecular density are not necessarily synonymous with bone loss and microstructural deterioration. *JBMR Plus*, 3, e10078. https://doi.org/10.1002/jbm4.10078

Zebaze, R.M., Ghasem-Zadeh, A., Bohte, A., Iuliano-Burns, S., Mirams, M., & Price, R.I. (2010) Intracortical remodelling and porosity in the distal radius and post-mortem femurs of women: A cross-sectional study. *Lancet*, 375, 1729–1736. https://doi.org/10.1016/S0140-6736(10)60320-0

How to cite this article: Schmidutz F, Milz S, Schiuma D, Richards RG, Windolf M, Sprecher CM. Cortical parameters predict bone strength at the tibial diaphysis, but are underestimated by HR-pQCT and µCT compared to histomorphometry. *J. Anat*. 2021;238:669–678. https://doi.org/10.1111/joa.13337